

BEHAVIOR OF CFRP CONFINED RC COLUMNS UNDER AXIAL LOAD AND UNIAXIAL CYCLIC LATERAL LOADING

Marta Del Zoppo¹, Marco Di Ludovico², Alberto Balsamo² and Andrea Prota²

¹ Department of Engineering, University of Naples “Parthenope”
Centro Direzionale, Isola C4, Naples (Italy)
e-mail: marta.delzoppo@uniparthenope.it

² Department of Structures for Engineering and Architecture, University of Naples “Federico II”
Via Claudio 21, Naples (Italy)
{diludovi, abalsamo, aprota}@unina.it

Keywords: confinement, CFRP, RC columns, ductility, deformation capacity.

Abstract. *In recent years, the use of FRP wrapping of reinforced concrete (RC) members has been recognized as a reliable method for seismic retrofit of existing structures. The external confinement of existing RC columns with FRPs is a sound technique for increasing the columns ductility, by preventing brittle mechanisms such as bars buckling or post-yielding shear failures and by improving the mechanical properties of concrete due to the lateral confining effect. Several models have been developed for predicting the ultimate displacement capacity and the ductility of FRP confined RC columns, however the accuracy of predictions has not been well established yet. In this study, the experimental behavior of a RC column confined at the plastic hinge region with one ply of carbon fibers (CFRP) is firstly analyzed and compared with the response of the unstrengthened control column. The specimens are cantilevers loaded with a low compressive axial load and subjected to uniaxial cyclic horizontal displacements. The responses of the columns have been analyzed and compared in terms of failure modes and strength and deformation capacity. Particular attention has been focused on the strain distribution recorded on the CFRP strips used to confine the RC column end; the strain profiles along the cross-section perimeter in case of axial load and bending moment interaction are presented and discussed at different load levels. In the second part of the study, the deformation capacity of FRP confined RC column is analytically obtained, by using models for FRP confined square columns available in literature. The comparison between analytical and experimental results showed that currently available models give conservative predictions of ultimate deformation capacity of confined columns.*

1 INTRODUCTION

Recent earthquakes confirmed the high vulnerability of existing reinforced concrete (i.e. RC) structures to seismic event, due to the lack of proper seismic detailing. To overcome the common deficiencies of RC members derived from the use of non-seismic design criteria, the use of fiber reinforce polymers (i.e. FRP) has been recognized as a reliable method for increasing members capacity [1-4]. In case of RC columns, mainly subjected to axial load and horizontal cyclic displacements, the ultimate deformation capacity can be increased by using an external confinement at the member's end, where the plastic hinge region is located, with unidirectional fibers orthogonal to the member longitudinal axis [5-10]. Indeed, the external confinement prevents mechanisms that can limit the ductility, such as longitudinal bars buckling, bond failure of lap-spliced reinforcement, and increases the ultimate strain of compressed concrete, enhancing the ductility of the member.

Several analytical models for the stress-strain relationship of FRP confined concrete subjected to axial compression have been developed in literature [11-16]. Two stress-strain models for FRP confined concrete [17, 18] were also implemented in the open-source platform OpenSees [19]. Nevertheless, most of them are developed for circular members and only a few models are available for square and rectangular sections. Moreover, differently from the case of pure compression, in presence of combined axial load and bending moment a gradient of concrete lateral dilatation occurs, because a part of the cross-section is in tension. Only few authors investigated on the effectiveness of confinement and on the mechanical properties of confined concrete in case of eccentric axial load [20-23].

Stress-strain models for FRP confined concrete can be used for predicting the ultimate deformation capacity of strengthened columns and for supporting the design of the retrofit intervention. However, few comparisons have been found in literature between analytical predictions and experimental results that validate the reliability of such models [16, 24].

In the first part of this study the experimental behavior of a square RC column confined at the plastic hinge region with one layer of carbon fibers (CFRP) is presented and discussed in comparison with a control column, which achieved a shear failure after the flexural yielding. The specimens were cantilevers loaded with a low compressive axial load and subjected to cyclic horizontal displacements. The responses of the columns have been analyzed in terms of failure modes and increased deformation capacity in case of external CFRP confinement. Particular attention has been focused on the increased deformation capacity (i.e. ultimate drift and ductility) due to the external wrapping with respect to the control column. Moreover, in order to investigate on the effectiveness of CFRP confinement in case of axial load and bending moment interaction, a detailed analysis related to the axial strains distribution along the fibers is reported.

The second part of the study presents the analytical predictions about the behavior of FRP confined column, obtained making use of the analytical stress-strain relationships found in literature and the plastic hinge concept. The comparison between analytical predictions and experimental results showed a conservative trend of analytical predictions of ultimate deformation capacity of retrofitted columns.

2 EXPERIMENTAL STUDY

2.1 Specimens geometry and material properties

Two square RC columns were designed in order to attain a brittle behavior after the flexural yielding, due to the reduction of shear capacity caused by the increasing ductility demand (i.e. flexure-shear failure mode).

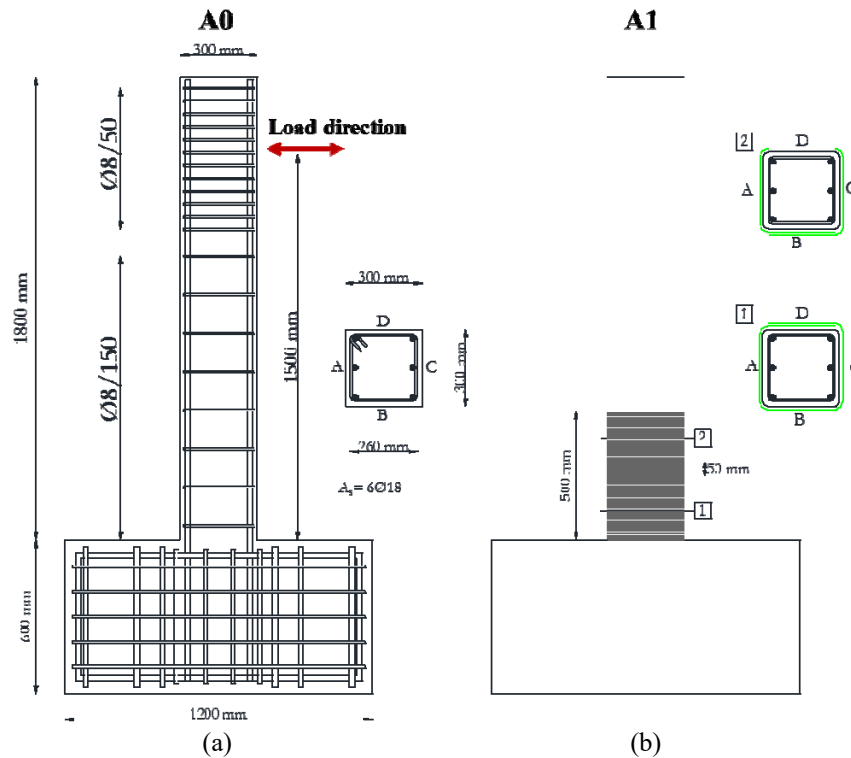


Figure 1: Geometry of specimens: control specimen (a) and CFRP confined specimen (b).

Each specimen had a square cross-section 300 x 300 mm reinforced with six 18 mm diameter deformed rebars along the column principal direction (longitudinal geometrical reinforcement ratio, $\rho_l = A_s/bh = 1.7\%$ with A_s total area of longitudinal steel reinforcement and b, h , cross section dimensions). No additional longitudinal reinforcement, which could help in shear resisting mechanism, was provided in the column secondary directions as typically found in existing structures. Transverse reinforcement was made of 8 mm diameter ties, spaced at 150 mm apart (transverse geometrical reinforcement ratio, $\rho_w = A_w/b_s = 0.22\%$ with A_w total area of transverse steel reinforcement and s the spacing). A reduced spacing has been adopted in the zone of load application to avoid localized damages. The geometrical properties and reinforcement detailing reported for the two specimens in Figure 1.

The specimens were cantilevers made by a column and a foundation block: the column height was 1,800 mm, the foundation block was 1,200 x 1,200 x 600 mm. The foundation block and the columns of each specimen were cast in two phases to reproduce the discontinuity of concrete at the column-foundation interface, as common practice in concrete casting procedures. The lateral load was applied at a distance of 1,500 mm from the foundation block, in order to simulate the behavior of a typical 3,000 mm height column, assuming that shear length L_s was the column mid-eight (i.e. $L_s = 1,500$ mm).

One of the two specimens (named **A0**) was used as a control specimen whereas the other (named **A1**) was confined at the column base with uniaxial CFRP sheets with fibers perpendicular with respect to the column longitudinal axis. The confinement was extended for 500 mm from the column-foundation interface, where the plastic hinge usually is developed. The radius of rounded corners is $R = 20$ mm. The column **A1** was confined with one layer of CFRP, with a thickness of dry fibers $t_f = 0.33$ mm. Since the CFRP sheets width was 300 mm, two sheets have been used for the confinement, with a 50 mm vertical overlap region located at the mid height of the confined zone. Further details of CFRP jacketing are reported in Figure 1b.

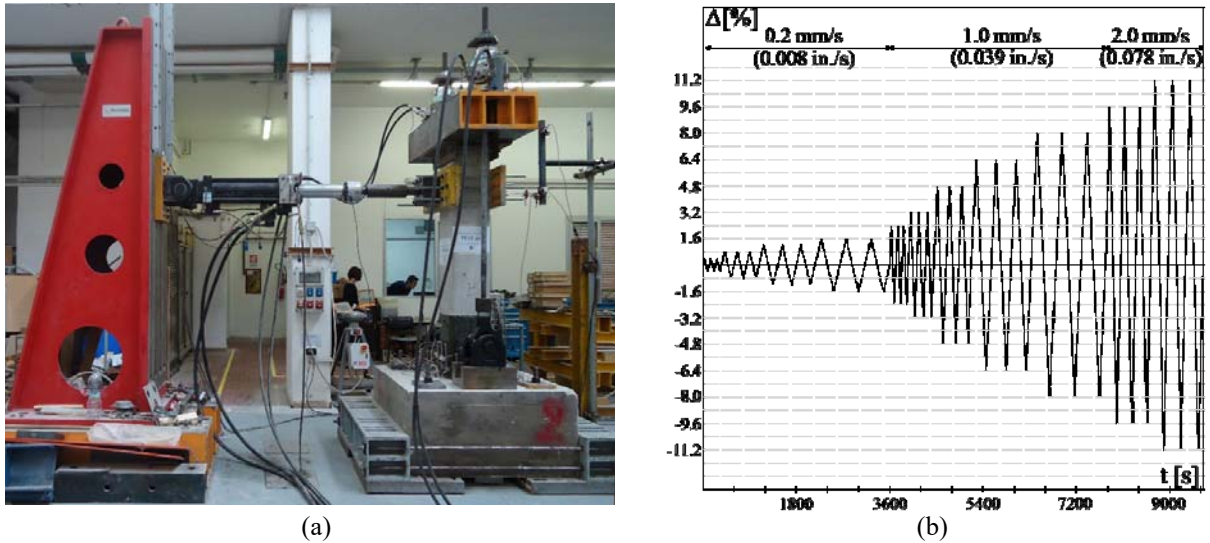


Figure 2: Test setup (a) and displacement protocol (b).

The average concrete compressive strengths, derived from compression tests on four concrete cylinders for each specimen, were $f_c = 16.3$ MPa and $f_c = 14.9$ MPa for columns **A0** and **A1**, respectively. The same class of steel has been used for longitudinal and transverse reinforcement, characterized by an average yielding strength $f_y = 531$ MPa. The average tensile modulus and minimum ultimate strain of carbon fibers given by the manufacturer are $E_f = 230$ GPa and $\varepsilon_{fu} = 1.3\%$, respectively. The CFRP sheets unit weight was 600 g/m^2 .

2.2 Test setup and instrumentation

The columns were subjected to constant axial load and horizontal cyclic loads. The test setup and instrumentation are described in detail in [25] and shown in Figure 2a. All the specimens were subjected to a constant axial load ratio ($\nu = N / A_c f_c$, where N is the axial load, A_c is the concrete gross area and f_c is the mean cylindrical concrete strength) equal to 0.1 and a lateral cyclic loading under displacements control, see Figure 2b. A displacement rate of 0.2 mm/s was used for initial four cycles, then a higher rate 1.0 mm/s was adopted for the next five cycles and a rate 2.0 mm/s was used for the last cycles. In each cycle, the target displacement was achieved three times, see Figure 2b.

3 DISCUSSION OF EXPERIMENTAL RESULTS

The experimental force-drift relationships recorded for the two tests are reported in Figure 3. The control specimen **A0** achieved a peak force $F_{max} = +86.1$ kN and $F_{max} = -85.4$ kN in the positive and negative direction, respectively (see Figure 3a). The drift ratio ($\Delta = d / L_s$ with d equal to the top column horizontal displacement and L_s the shear length) at the peak load was $\Delta_{F_{max}} = 4.8\%$ both in the positive and negative load action directions. During the cycle at $\Delta = 6.4\%$, a sudden decrease of strength and stiffness has been observed among the three consecutive repetitions and the loading branch of the next cycle, so that the test was stopped. Thus, the ultimate drift ratio has been assumed equal to the one of last cycle, $\Delta_{0.8F_{max}} = \pm 6.4\%$, cause a strength degradation of 20% of the peak force (i.e. a lateral force lower than 80% of the maximum one) has not been achieved. At a drift ratio of 1.6%, diagonal cracks appeared along the sides B-D parallel to the load action direction especially in the plastic hinge region. During the cycles at imposed drift of 4.8%, the first concrete spalling has been observed along

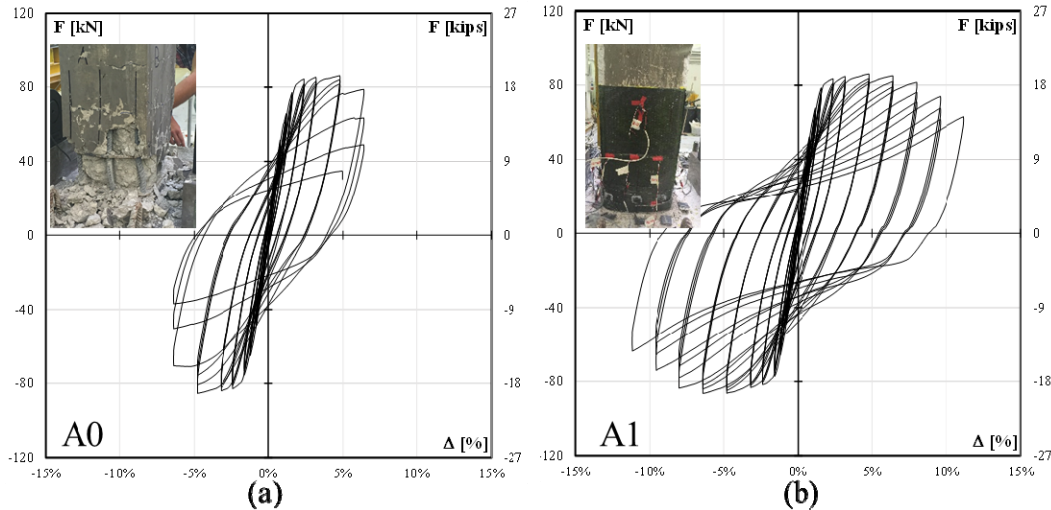


Figure 3: Force-Drift curves for control column A0 (a) and column A1 confined with one ply of CFRP (b).

the side A of the specimen. At this stage, the buckling of longitudinal bars was also detected. At failure, the concrete cover was completely spalled off; the spalling of concrete involved a region with a height of about 470 mm from the fixed end. As expected, the failure mode of specimen **A0** was “quasi-ductile”, since plastic deformations were attained before a premature failure due to the reduced shear capacity in the plastic hinge region.

A similar response in terms of peak forces has been recorded on specimen **A1** confined with one ply of CFRP, so no increase of global strength has been recorded. However, the global deformation and energy dissipation capacity was strongly improved by means of the CFRP wrapping, see Figure 3b. In particular, the experimental peak forces were $F_{max} = +86$ kN and $F_{max} = -86.5$ kN in the positive and negative direction, respectively. Also in this case, the drift corresponding at the peak loads was $\Delta_{F_{max}} = 4.8\%$ both in the positive and negative load action directions. By contrast, the ultimate conventional drift ratio, corresponding to a strength degradation of 20% of the peak force, was significantly greater than in the case of **A0** test and equal to $\Delta_{0.8F_{max}} = \pm 10.4\%$. Thus, the brittle mechanism observed in the control specimen was prevented by the external confinement and a pure flexural behavior has been attained. However, at a drift ratio of 6.4%, some diagonal cracks were detected in the unconfined region along the B-D sides of the specimen. At failure, the confined concrete was totally cracked. No CFRP tensile failure or debonding have been observed, but a premature failure given by horizontal cracks between fibres was detected. In particular, longitudinal cracks along the fibres direction developed at about 50 mm from the fixed-end, due to a concentration of stresses provided by the lateral dilatation of damaged concrete in the direction orthogonal to the fibres.

Thus, the CFRP confinement of the specimen increased the ultimate deformation capacity of +62.4% with respect to the control specimen.

4 PREDICTION OF ULTIMATE DRIFT

4.1 Analytical approach

Analytical models and predictive equations for defining a simplified force-drift curve of FRP confined RC columns are herein investigated. The envelope curve of cyclic response of the confined RC columns can be approximated with a bilinear curve, which consists of a three

data points: the origin, the point corresponding to the first yielding of internal steel reinforcement and the point corresponding to the ultimate deformation capacity at flexural failure.

The elastic drift corresponding to the first yielding of internal steel rebars, Δ_y , can be calculated according to the formulation suggested in [16], which account for the flexural and shear deformations and for the fix-end rotation before the yielding:

$$\Delta_y = \frac{1}{3}\phi_y (L_s + 0.5z) + 0.0014 \left(1 + 1.5 \frac{h}{L_s}\right) + 0.125\phi_y \frac{d_b f_y}{\sqrt{f_c}} \quad (1)$$

where $\phi_y = 2\varepsilon_y/h$ the simplified yielding curvature, z the internal lever arm and d_b the longitudinal steel bars diameter.

The ultimate deformation capacity is calculated as the sum of the elastic drift ratio, Δ_y , and the plastic one, Δ_{pl} . Two different approaches reported Biskinis and Fardis (2013) [16] can be followed for evaluating the plastic drift ratio: (i) by using an empirical formulation calibrated on 219 experimental tests on FRP confined members and reported in Eq. (2) or (ii) by using a mechanical formulation based on the plastic hinge concept and reported in Eq. (3).

$$\Delta_{pl,emp.} = 0.0088 \left(1 + \frac{1}{1.6}\right) (0.25)^{\nu} \left(\frac{\max(0.01; \omega')}{\max(0.01; \omega)}\right)^{0.3} f_c^{0.2} \left(\frac{L_s}{h}\right)^{0.35} 25^{\left[\frac{\alpha_w \rho_w f_y}{f_c} + \left(\frac{\alpha_f \rho_f E_f \varepsilon_{f,eff}}{f_c}\right)_{eff}\right]} 1.275^{100\rho_l} \quad (2)$$

$$\Delta_{pl,mech.} = (\phi_u - \phi_y) L_p \left(1 - 0.5 \frac{L_p}{L_s}\right) + 5d_b (\phi_u + \phi_y) \quad (3)$$

where α_w and α_f are factors accounting for the effectiveness of confinement for steel and FRP reinforcement, respectively, ϕ_u is the ultimate curvature and L_p is the plastic hinge length. The last term of Eq. (3) represents the post-elastic fixed-end rotation, empirically obtained as best fitting of experimental results on unconfined members. A further description of the aforementioned formulations can be found in [16].

The plastic hinge length is herein calculated as reported in [16] in case of cyclic loading for unconfined members:

$$L_p = 0.2h \left[1 + \frac{1}{3} \min\left(9; \frac{L_s}{h}\right)\right] \quad (4)$$

The lateral force corresponding to the elastic curvature and the ultimate curvature, corresponding to the achievement of an ultimate concrete compressive strain, are calculated performing a moment-curvature analysis for the column critical cross-section by using a fiber model [26]. For the non-circular FRP confined concrete, six stress-strain models were selected from the international codes provisions and recent literature: *fib* Bulletin 14 – Spoelstra and Monti (2001) [27], ACI 440 (2008) [28], CNR DT-200 (2013) [29], Biskinis and Fardis (2013) [16], Pantazopoulou et al. (2016) [30] and Ghatte et al. (2017) [24]. The main expressions for ultimate strength, f_{cu} , and strain, ε_{cu} , of FRP confined concrete according to selected models are reported in Table 1 as a function of the unconfined concrete peak strength and corresponding strain, f_{c0} and ε_{c0} . The effective lateral confinement pressure, f_l' , exerted by the FRP confinement is calculated as:

$$f_l' = \alpha_f \rho_f E_f \varepsilon_{f,eff} \quad (5)$$

where α_f is the FRP effectiveness of confinement factor, ρ_f is geometrical ratio of FRP external reinforcement and $\varepsilon_{f,eff} = k_{eff} \varepsilon_{fu}$ is the FRP effective strain.

Since the main purpose of the analysis is the evaluation of the ultimate curvature under combined axial load and bending moment, the concrete stress-strain relationships were considered as follows: the first part is parabolic up to the peak strength of unconfined concrete (strength equal to the experimental $f_{c0} = f_c$ and conventional strain at peak strength $\varepsilon_{c0} = 0.002$); the second part is linear up to the ultimate strength and strain calculated as reported in Table 1. For steel internal reinforcement, an elasto-plastic model has been selected.

In order to compare the different stress-strain models for FRP confined concrete, the ultimate strength and deformations calculated according to the expressions in Table 1 are summarized in Table 2, along with the limitation adopted in each model for the FRP effective strain $\varepsilon_{f,eff}$ and k_{eff} . The stress-strain relationships for the FRP confined concrete are also plotted in Fig. 7.

Model	f_{cu}/f_{c0}	$\varepsilon_{cu}/\varepsilon_{c0}$
<i>fib</i> Bulletin 14 (2001)	$0.2 + 3(f_l'/f_{c0})^{0.5}$	$2 + 1.25\varepsilon_{f,eff}(E_c/f_{c0})(f_l'/f_{c0})^{0.5}$
ACI 440.2R (2008)	$1 + 3.3f_l'/f_{c0}$	$1.5 + 12(f_l'/f_{c0})(\varepsilon_{f,eff}/\varepsilon_{c0})^{0.45}$
CNR DT-200 (2013)	1	$(0.0035 + 0.015(f_l'/f_{c0})^{0.5})/\varepsilon_{c0}$
Biskinis and Fardis (2013)	$1 + 3.3f_l'/f_{c0}$	$(0.0035 + (10/h)^2 + 0.4f_l'/f_{c0})/\varepsilon_{c0}$
Pantazopoulou et al. (2016)	0.85	$(0.0035 + 0.075(\alpha_w\rho_w f_y + f_l')/f_{c0})/\varepsilon_{c0}$
Ghatte et al. (2017)	$1 + 2.54f_l'/f_{c0}$	$1 + (h/b)19.27(f_l'/f_{c0})^{0.53}$

Table 1: Expressions for FRP confined concrete ultimate strength and strain (f_{c0} and ε_{c0} are the peak strength and strain of unconfined concrete).

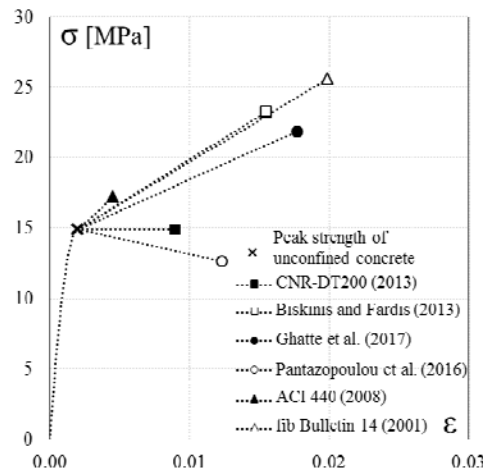


Figure 7: Stress-strain models for FRP confined concrete.

	<i>fib</i> Bulletin 14 (2001)	ACI 440 (2008)	CNR 200 (2013)	Biskinis and Fardis (2013)	Pantazopoulou et al. (2016)	Ghatte et al. (2017)	Empiric form Eq. (2)
ε_{cu}	0.0199	0.0045	0.0090	0.0155	0.0123	0.0177	-
f_{cu} [MPa]	25.6	17.2	14.9	-	12.7	21.9	-
k_{eff}	0.58	0.31	0.60	0.58	0.70	0.85	1
$\varepsilon_{f,eff}$	0.008	0.004	0.008	0.008	0.009	0.011	0.013

Table 2: Main parameters calculated for selected models.

From the comparison among different axial stress-strain models for FRP confined concrete, see Figure 7, it is observed that most of them assume a hardening behavior up to the failure, due to the elastic behavior of FRP material [i.e. *fib* Bulletin 14 – Spoelstra and Monti (2001), ACI 440 (2008), Biskinis and Fardis (2013), Ghatte et al. (2017)]. The model proposed by CNR DT-200 (2013) for evaluating the ultimate drift or chord rotation is a parabolic-rectangular model, with ultimate strain increased by the FRP confining effect. On the contrary, the model proposed by Pantazopoulou et al. (2016) for FRP confined concrete is similar to that of concrete confined by steel hoops, with a descending branch after the peak. Moreover, the model proposed by Pantazopoulou et al. (2016) takes into account also the confinement provided by internal transverse steel reinforcement.

4.2 Comparison between experimental, analytical and numerical results

Firstly, the experimental behavior of control column **A0** has been compared with the analytical predictions given by Eq. (2) and Eq. (3) in case of steel confinement only, in order to evaluate the reliability of the approaches. For the unconfined concrete, a Mander [31] model has been used with a concrete ultimate compressive strain of 0.004. The experimental force-drift curve is reported in Figure 8 along with the experimental envelope curve, the analytical bilinear curve obtained within Eq. (2) and the analytical bilinear curve obtained by using Eq. (3). In particular, Figure 8a reports the analytical curve obtained by using Eq. (2), whereas Figure 8b shows the analytical curve obtained by using Eq. (3).

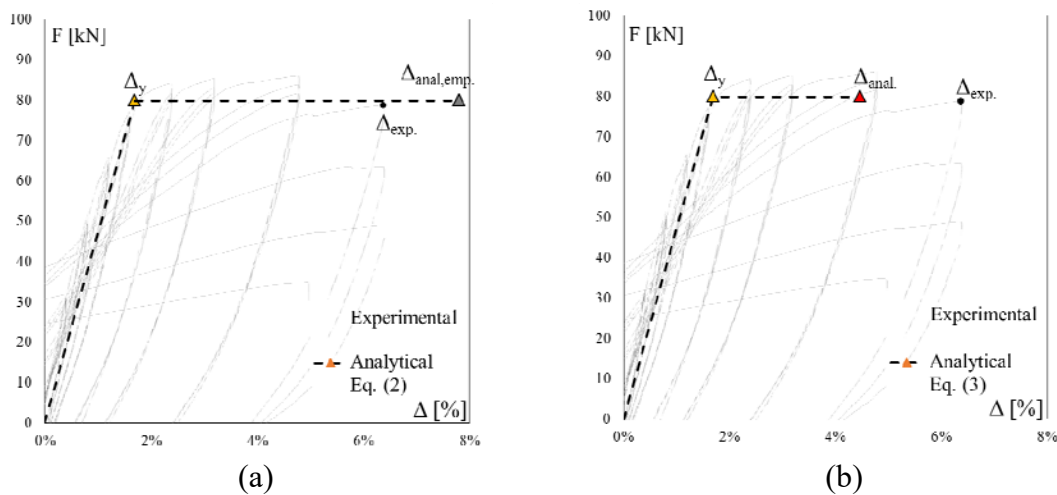


Figure 8: Comparison of experimental, analytical (Eq. (2) and Eq. (3)) results for control specimen A0.

For the control specimen **A0**, the limitation of concrete ultimate strain to 0.004 leads to conservative predictions (i.e. -30%) of ultimate deformation capacity for the analytical approach based on curvatures. Conversely, the analytical approach based on empirical formulation in Eq. (2) overestimated the deformation capacity of the member of +22%. The main results in terms of ultimate deformation capacity obtained for specimen **A0** are summarized in Table 3 ($\Delta_{exp.}$ experimental ultimate drift, $\Delta_{anal.}$ analytical drift according to Eq. (3), $\Delta_{anal.emp.}$ ultimate drift according to empiric formulation in Eq. (2)).

$\Delta_{exp.}$	$\Delta_{anal.emp.}$ (Eq. (2))	Error	$\Delta_{anal.}$ (Eq. (3))	Error
6.4%	7.8%	+22%	4.5%	-30%

Table 3: Predictions of ultimate drift ratio for control specimen A0.

However, it should be noted that the ultimate flexural drift ratio of control specimen has not been achieved during the test, due to the premature brittle failure that is not taken into account in these analytical approaches.

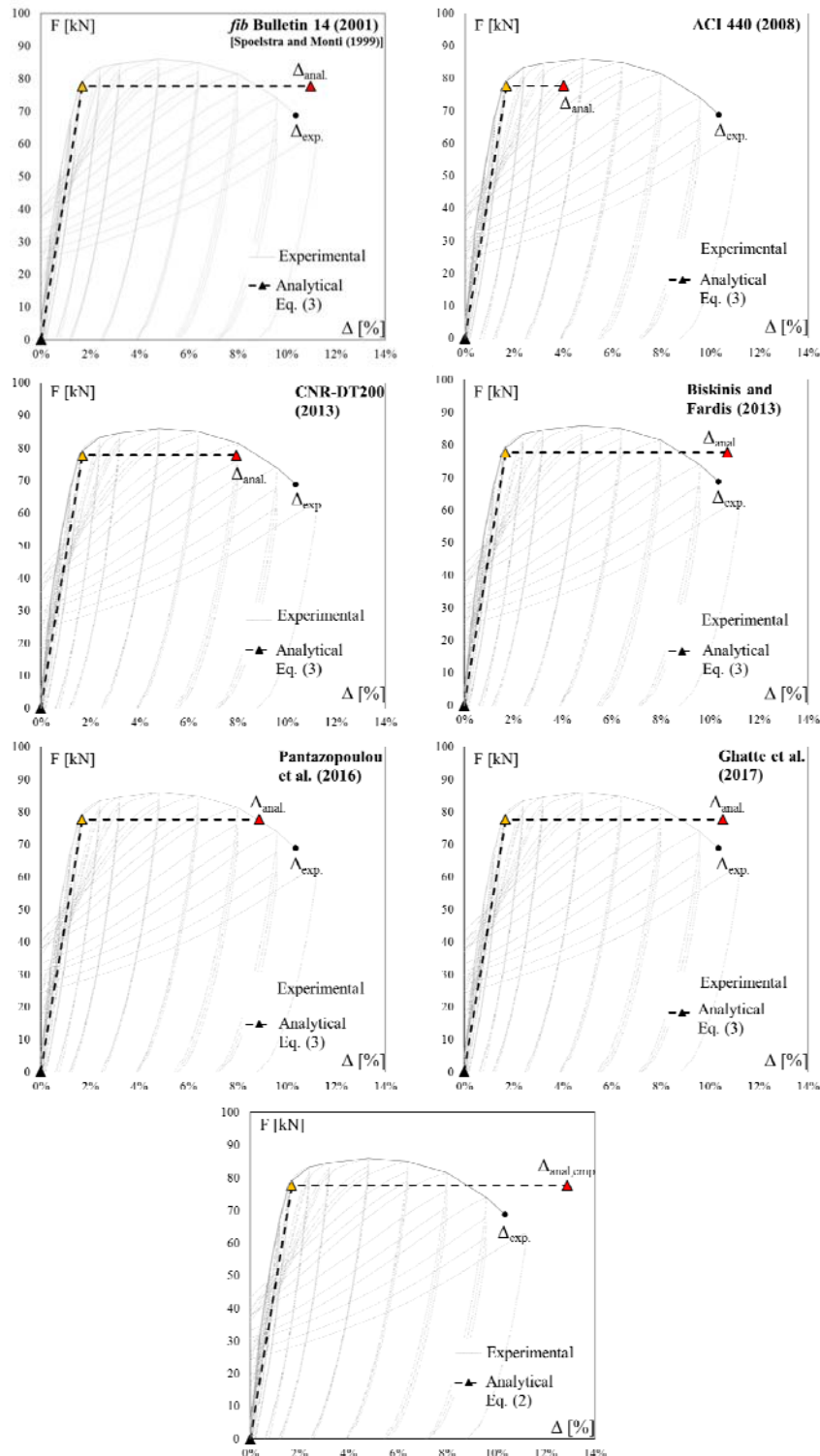


Figure 9: Comparison of experimental and analytical force-drift curves for specimen A1 according to different stress-strain FRP confined concrete models.

Model	Δ_{exp}	Δ_{anal}	Error	$\Delta_{anal,emp.}$	Error
<i>fib</i> Bulletin 14 (2001)		11.0%	+6%		
ACI 400 (2008)		4.0%	-61%		
CNR-DT200 (2013)	10.4%	7.9%	-23%	12.9%	+25%
Biskinis et al. (2013)		10.7%	+3%		
Pantazopoulou et al. (2016)		8.9%	-14%		
Ghatte et al. (2017)		10.5%	+2%		

Table 4: Prediction of ultimate drift for control specimen A1.

The main results in terms of ultimate deformation capacity for FRP confined specimen **A1** are summarized in Table 4 for selected models.

The comparison between experimental and analytical results based on plastic hinge concept (i.e. derived from Eq. (3)) shows that the adoption of stress-strain models proposed by ACI 440 (2008), CNR DT-200 (2013) and Pantazopoulou et al. (2016) for calculating the ultimate drift ratio of the confined column under cyclic loading give results sensitively lower than the experimental one (i.e. errors of -61%, -23% and -14% respectively). Conversely, models proposed by Ghatte et al. (2017), Biskinis and Fardis (2013) and *fib* Bulletin 14 (2001) give results more close to the experimental ultimate drift ratio (i.e. errors of +2%, +3% and +6%, respectively). On the other hand, the empirical approach based on regression of experimental results (i.e. derived from Eq. (2)) gives a non-conservative result and overestimates the ultimate capacity of the confined member of +25%. This result is consistent with the CoV declared by the authors in [16] for the empirical formulation in Eq. (2) equal to $\pm 30.6\%$.

5 CONCLUSIONS

The experimental behavior of a RC column subjected to combined axial load and cyclic uniaxial bending and confined at the plastic hinge region with CFRP uniaxial sheets has been presented and discussed in comparison with an unconfined control specimen. The confinement of the potential plastic hinge region did not changed the member strength capacity but prevented the brittle failure observed in the control specimen and significantly increased its deformation capacity (+60.4%), due to the external lateral compression exerted by the fibers.

Then, analytical approaches provided by international codes and recent literature for predicting the ultimate drift ratio of confined members have been analyzed and applied for the specimen experimentally tested. The comparison between the experimental result of the column confined with FRP and the analytical results, according to plastic hinge concept, shows that the stress-strain models for confined concrete proposed by ACI 440 (2008) strongly underestimate the ultimate deformation capacity (-61%) whereas the models proposed by *fib* Bulletin 14 (2001), Biskinis and Fardis (2013), Ghatte et al. (2017) give a good prediction of ultimate drift ratio, with errors lower than +6%. On the other hand, the empirical approach based on regression of experimental results overestimated the ultimate drift ratio of confined specimen of 25%. All the results are based on a single experimental tests and can not be generalized for CFRP confined RC members.

ACKNOWLEDGEMENTS

This study was performed in the Framework of PE 2014-2016; joint program DPC-Reluis Task 1.2: Seismic capacity of RC structural members: beams, columns, beam-column joints and shear walls.

REFERENCES

- [1] H. Katsumata, Y. Kobatake, T. Takeda, A study on strengthening with carbon fiber for earthquake-resistant capacity of existing reinforced concrete columns. *Ninth World Conference on Earthquake Engineering*, 1988.
- [2] H. Saadatmanesh, M.R. Ehsani, M.W. Li, Strength and Ductility of Concrete Columns Externally Reinforced with Fiber Composite Straps. *ACI Structural Journal*, **91**, 434-447, 1994.
- [3] A. Nanni, M. Norris, FRP jacketed concrete under flexure and combined flexure-compression. *Construction and Building Materials*, **9**(5), 273-281, 1995.
- [4] F. Seible, M.J.N. Priestley, G.A. Hegermier, D. Innamorato, Seismic retrofit of rc columns with continuous carbon fiber jackets. *Journal for Composites for Construction*, **1**(2), 52-62, 1997.
- [5] R.D. Iacobucci, S.A. Sheikh, O. Bayrak, Retrofit of square concrete columns with carbon fiber-reinforced polymer for seismic resistance. *ACI Structural Journal*, **100**(6), 785-794, 2003.
- [6] M.H. Harajli, Z. Khalil, Seismic FRP retrofit of bond-critical regions in circular RC columns: validation of proposed design methods. *ACI Structural Journal*, **105**(6), 760, 2008.
- [7] M. Di Ludovico, G. Manfredi, E. Mola, P. Negro, A. Prota, Seismic Behavior of a Full-Scale RC Structure Retrofitted Using GFRP Laminates. *ASCE – Journal of Structural Engineering*, **134**(5), 810-821, 2008.
- [8] M. Di Ludovico, A. Balsamo, A. Prota, G. Manfredi, Comparative Assessment of Seismic Rehabilitation Techniques on a Full-Scale 3-Story RC Moment Frame Structure. *Structural Engineering and Mechanics*, **28**(6), 727-747, 2008.
- [9] O. Ozcan, B. Binici, G. Ozcebe, Seismic strengthening of rectangular reinforced concrete columns using fiber reinforced polymers. *Engineering Structures*, **32**(4), 964-973, 2010.
- [10] H.F. Ghatte, M. Comert, C. Demir, A. Ilki, Seismic performance of full-Scale FRP Retrofitted substandard RC Columns Loaded In The Weak Direction. *Applied Mechanics & Materials*, **847**, 2016.
- [11] M. Samaan, A. Mirmiran, M. Shahawy, Model of concrete confined by fiber composites. *ASCE – Journal of Structural Engineering*, **124**, 1025–1031, 1998.
- [12] L. Lam, J.G. Teng, Design-oriented stress-strain model for FRP-confined concrete in rectangular columns. *J. Reinf. Plast. Compos*, **22**, 1149–1186, 2003.
- [13] M.H. Harajli, Axial stress-strain relationship for FRP-confined circular and rectangular concrete columns. *Cem. Concr. Compos*, **28**, 938–948, 2006.
- [14] G.P. Lignola, A. Prota, G. Manfredi, E. Cosenza, Unified theory for confinement of RC solid and hollow circular columns. *Compos. Part B*, **39**, 1151–1160, 2008.
- [15] M. Di Ludovico, A. Prota, G. Manfredi, Structural upgrade using basalt fibers for concrete confinement. *Journal of composites for construction*, **14**(5), 541-552, 2010.

- [16] D. Biskinis, M.N. Fardis, Models for FRP-wrapped rectangular RC columns with continuous or lap-spliced bars under cyclic lateral loading. *Eng. Struct.*, **57**, 199–212, 2013.
- [17] F. Braga, R. Gigliotti, M. Laterza, Analytical stress–strain relationship for concrete confined by steel stirrups and/or FRP jackets. *Journal of structural engineering*, **132**(9), 1402-1416, 2006.
- [18] K.G. Megalooikonomou, G. Monti, S. Santini, Constitutive model for fiber-reinforced polymer-and tie-confined concrete. *ACI Structural Journal*, **109**(4), 569, 2012.
- [19] S. Mazzoni, F. McKenna, M.H. Scott, G.L. Fenves, OpenSees command language manual. *Pacific Earthquake Engineering Research (PEER) Center*, 2006.
- [20] A. Parvin, W. Wang, Behavior of FRP jacketed concrete columns under eccentric loading. *Journal of Composites for Construction*, **5**(3), 146-152, 2001.
- [21] M.N.S. Hadi, Behaviour of FRP wrapped normal strength concrete columns under eccentric loading. *Composite Structures*, **72**, 503-511, 2006.
- [22] J.Y. Park, Y.H. Lee, A. Scanlon, Confined concrete model for columns under combined axial load and bending. *Mag. Concr. Res.*, **64**, 827–836, 2012.
- [23] Y.F. Wu, C. Jiang, Effect of load eccentricity on the stress–strain relationship of FRP-confined concrete columns. *Compos. Struct.*, **98**, 228–241, 2013.
- [24] H. Ghatte, M. Comert, C. Demir, A. Ilki, Evaluation of FRP Confinement Models for Substandard Rectangular RC Columns Based on Full-Scale Reversed Cyclic Lateral Loading Tests in Strong and Weak Directions. *Polymers*, **8**(9), 323, 2017.
- [25] M. Di Ludovico, G. Verderame, A. Prota, G. Manfredi, E. Cosenza, Cyclic Behavior of Nonconforming Full-Scale RC Columns. *Journal of Structural Engineering*, 2013.
- [26] M. Del Zoppo, M. Di Ludovico, A. Ghersi, Behaviour of non-conforming rc members under compressive axial load and biaxial bending. *5th ECCOMAS thematic conference on computational methods in structural dynamics and earthquake (COMPdyn 2015)*, Crete, Greece, 2015.
- [27] *fib Bulletin 14*. Externally bonded FRP reinforcement for RC structures. CH-1015, Lausanne, 2001.
- [28] Guide for Design and Construction of Externally Bonded FRP Systems for Strengthening Concrete Structures, ACI 440.2R-08, ACI: Farmington Hills, MI, USA, 2008.
- [29] Consiglio Nazionale Delle Ricerche (CNR). Instructions for design, execution and control of strengthening interventions through fiber-reinforced composites. CNR-DT 200-13, Consiglio Nazionale delle Ricerche, Rome, Italy; 2013.
- [30] S.J. Pantazopoulou, S.P. Tastani, G.E. Thermou, T. Triantafillou, G. Monti, D. Bournas, M. Guadagnini, Background to the European seismic design provisions for retrofitting RC elements using FRP materials. *Structural Concrete*, **17**(2), 194-219, 2016.
- [31] J.B. Mander, M.J. Priestley, R. Park, Theoretical stress-strain model for confined concrete. *Journal of structural engineering*, **114**(8), 1804-1826, 1988.